

10th CIRP Conference on Photonic Technologies [LANE 2018]

## Weld pool shape observation in high power laser beam welding

Antoni Artinov<sup>a</sup>, Nasim Bakir<sup>a,\*</sup>, Marcel Bachmann<sup>a</sup>, Andrey Gumenyuk<sup>a</sup>, Michael Rethmeier<sup>a</sup><sup>a</sup>BAM Federal Institute for Materials Research and Testing, Unter den Eichen 87, Berlin 12205, Germany\* Corresponding author. Tel.: +49 3081044622; E-mail address: [Nasim.Bakir@bam.de](mailto:Nasim.Bakir@bam.de)

### Abstract

The geometry of the melt pool in laser beam welding plays a major role to understand the dynamics of the melt and its solidification behavior. In this study, a butt configuration of 15 mm thick structural steel and transparent quartz glass was used to observe the weld pool geometry by means of high-speed camera and an infrared camera recording. The observations show that the dimensions of the weld pool vary depending on the depth. The areas close to the weld pool surface take a teardrop-shape. A bulge-region and its temporal evolution were observed approximately in the middle of the depth of the weld pool. Additionally, a 3D transient thermal-fluid numerical simulation was performed to obtain the weld pool shape and to understand the formation mechanism of the observed bulging effect. The model takes into account the local temperature field, the effects of phase transition, thermo-capillary convection, natural convection and temperature-dependent material properties up to evaporation temperature. The numerical results showed good accordance and were furthermore used to improve the understanding of the experimentally observed bulging effect.

© 2018 The Authors. Published by Elsevier Ltd. This is an open access article under the CC BY-NC-ND license

<https://creativecommons.org/licenses/by-nc-nd/4.0/>

Peer-review under responsibility of the Bayerisches Laserzentrum GmbH.

**Keywords:** high power laser beam welding; transient weld pool shape; bulging; numerical process simulation

### 1. Introduction

These days the high power laser beam welding technology has become an established tool for increasing productivity in thick-plate welding. With available laser powers of up to 100 kW for solid states lasers, the possible thickness of specimens to be welded by a single pass welding process has increased up to 50 mm [1, 2]. The comparison of this method with more traditional processes, such as Gas Metal Arc Welding (GMAW) and Submerged Arc Welding (SAW) shows the great potential offered by laser beam welding. The conventional methods mostly need multiple passes to achieve the desired welding depth, e.g. for the production of thick-walled pipelines for the oil and gas industry. The application of the laser beam welding replaces these methods by a single pass and provides the benefits of high efficiency, high reachable welding speed, high depth to width ratio and narrow heat affected zone [3].

The complicated physics behind the laser beam welding process and the number of the occurring physical phenomena

make the estimation of the most important process quantities such as the temperature profile and the shape of the weld pool very challenging. The same holds also for the appropriate choice of the relevant process parameters like welding speed, laser power and focal position.

The aim of the present work was the experimental and theoretical investigation of the resulting weld pool shape obtained by high power laser beam welding. The occurring phenomena in the weld pool shape are responsible for the formation of different defects, e.g. the formation of solidification cracks. In [4] it was shown that another identified factor, the so-called bulging of the weld, has a significant influence on the temperature field and mechanical stress distribution, which is contributing to the formation of hot cracking. These phenomena, bulging and hot cracking are related to each other by the delayed solidification at the rear part of the weld pool.

Recent numerical investigations show that the geometry of the melt pool is highly influenced by the dynamics of the molten material and its solidification behavior, see [5,6].

Experimental setup and numerical model are proposed to visualize the shape of the weld pool in the longitudinal section of the weld. For this a butt configuration of a transparent quartz glass and a low-alloyed steel was used. The same configuration of the experiments has been also used in Li *et al.* [7] in order to study the plasma and the keyhole behavior during high power deep penetration fiber laser beam welding of stainless steel. Zhang *et al.* [8] also successfully applied this method to study the zinc behavior during laser beam welding.

The aim of the present study was to investigate the geometry of the weld pool in the longitudinal section qualitatively. The weld pool shape was observed using a high-speed camera and an infrared camera. A depth dependency of the weld pool dimensions with a teardrop shape near the upper and bottom surface and a bulge-region approximately in the middle of the depth were observed. A simplified numerical simulation was used to reproduce the experimentally observed phenomena, which enabled the study of the formation mechanism of the bulging in the weld.

## 2. Numerical modelling

The numerical model proposed in this work was implemented and solved with the commercial Software ANSYS Fluent. The CFD (Computational Fluid Dynamics) process simulation of full-penetration keyhole laser beam welding was used to obtain the weld pool shape by taking into account the most important physical phenomena, such as the effects of phase transition, thermo-capillary convection, natural convection and temperature-dependent material properties up to evaporation temperature. The model has the geometrical dimensions of 70 mm x 10 mm x 15 mm and makes use of a symmetry plane, which reduces the computational effort and time. For the discretization of the computational domain, a polygonal mesh of tetrahedral and triangular elements was used. The domain was meshed by about  $1.1 \times 10^6$  elements and had a minimum element size of 0.1 mm at the free surfaces and the keyhole wall. Since strongly coupled physical aspects and highly nonlinear system of equations are needed to be considered for modelling of the laser beam welding process, a simplified form of the mathematical model was used in order to guarantee numerical stability and acceptable computing time. The main assumptions made in the model were similar to those used in [9, 10] and are given as follows:

- Quasi-steady-state approach.
- Adapted size of the computational domain.
- Fixed free surface geometry.
- A simplified and fixed keyhole geometry was used as a model parameter to adapt the numerical to the experimental results. Thus effects caused by keyhole oscillations were not considered.
- A turbulent flow pattern.
- Apparent heat capacity formulation was used to consider the amount of the fusion heat.
- Shear stress due to the interaction of metal vapor and liquid metal was not considered.

- Heat losses by radiation were neglected due to the high relation of volume versus surface of the plate.

The equations of mass and momentum conservation for incompressible flow, were used, as they are implemented within the simulation framework of ANSYS Fluent to obtain the velocity and pressure fields [11]. The laser material interaction (heat input) was considered by setting the keyhole surface to evaporation temperature. The buoyancy force driven by the deviation of the temperature dependent density was modelled by the well-known Boussinesq approximation [12]. The transition zone or also known as the “mushy zone” was considered by the Carman-Kozeny equation. This approach allows the modelling of the welding process as a single-phase by using a temperature dependent liquid-fraction, to calculate the amount of liquid in the element and distinguish between solid and liquid [13]. Additionally, a  $\kappa - \epsilon$  turbulence model was included in the transport equations. The needed constants were determined from experimental data, see [14].

The equations describing the behavior of the molten metal were strongly coupled with the equation of energy conservation [11]. Hence the influence of the convection on the energy transport and vice versa was considered. Here the heat conductivity was modified by the Kays-Crawford heat transport turbulence model [15] to account for the amount of turbulent heat conductivity. As last, the method of apparent heat capacity was used [16]. In this way, the amount of latent heat was released uniformly within the mushy zone. In the simulation, the phase change temperature range was chosen to be within a bandwidth of 50 K.

## 3. Experimental setup

Laser beam welding experiments were conducted on 15 mm thick structural steel (S355) and transparent quartz glass in a butt configuration. Welding was performed with a fibre laser at a focal position of -5 mm, laser power of 18 kW and a welding speed of 2 m/min. The schema of the experimental setup is shown in Fig. 1.

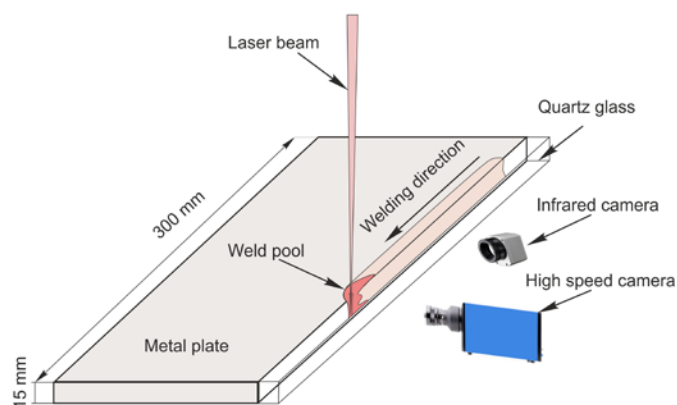


Fig. 1 Experimental setup

The laser spot was adjusted to be half on the steel plate and a half on the glass knowing that the glass is transparent for the laser wavelength of about  $1.06 \mu\text{m}$ . Simultaneously, the weld

pool has been observed using an infrared camera and a high-speed camera from the glass side.

The used detector in the infrared camera was able to detect the mid-wavelength infrared (MWIR), e.g. from 1  $\mu\text{m}$  up to 5  $\mu\text{m}$ . In this study, the used quartz glass had excellent transmission properties (up 90%) for wavelengths between 0.2  $\mu\text{m}$  and 2.5  $\mu\text{m}$ . This intersection between the spectral transmission of the glass and detecting range of the infrared camera allows monitoring the thermal profile of the welding pool through the glass. Due to the unique properties of the quartz glass such as low thermal conductivity, low thermal expansion coefficient, excellent thermal shock resistance and high melting temperature e.g. comparable to the used steel, the glass-steel interface can be considered as a plane of symmetry.

However, it must also be mentioned here that these experiments were carried out only to observe qualitatively the longitudinal geometry of weld pool.

#### 4. Results and Discussion

The high-speed observations (see Fig. 2) show that the dimensions of the melt vary depending on the depth. A mixture of vapor, laser reflections on the keyhole surfaces and a part of the melt were observed with help of the high-speed camera. In the top high-speed image in Fig. 2 can be seen that the observed bulge is located near, but outside the keyhole region. The infrared measurements confirmed the observations of the high-speed camera imaging (see Fig. 3). Hence this bright region defined by the yellow line represents an isotherm between the evaporation and the solidus temperatures. The observed bulge in the mixture should have, in his turn, influence on the solidification front. The longitudinal view of the weld pool shows that the material in the middle has a delay in the solidification.

The areas close to the weld pool surface take a teardrop-shape. Additionally, two necking areas were also detected, which were located between the bulge and the upper and lower weld pool regions. The assumed solidification front in the longitudinal direction approximately takes the qualitative shape of a quartic function.

However, the physical explanation of the origin of the lower and upper necking as well as the bulge can be better analysed with help of the numerical simulation.

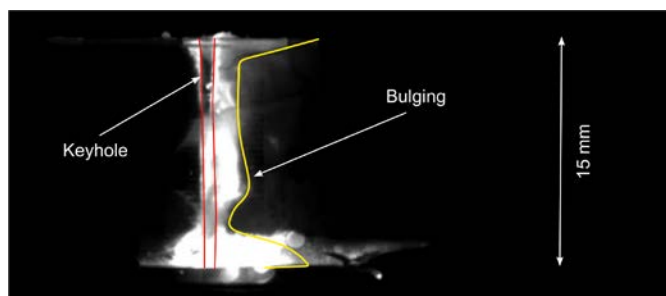


Fig. 2 Longitudinal view through the quartz glass using a high speed camera

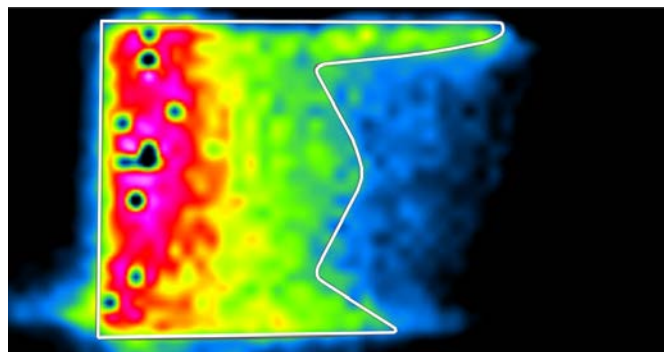


Fig. 3 Longitudinal view through the quartz glass using the infrared camera

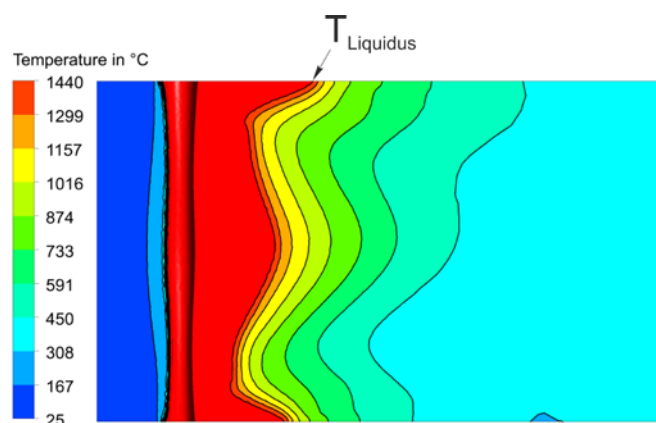


Fig. 4 Numerically calculated temperature field in the symmetry plane of the weld.

The presented model aims to predict the size and the shape of the melt pool in the steady-state zone of the weld. Thus the physical aspects with the highest impact on the heat and mass transfer, such as latent heat, buoyancy and Marangoni force are considered. The geometry of the three-dimensional weld pool is defined by the liquidus-temperature and can be seen in Fig. 4.

The thermocapillary convection on the upper and lower part of the specimen and the bulge in the middle of the plate are the main factors defining the end-shape of the weld pool. In total there are numerous flow directions in the molten metal, see Fig.5. All these form the weld pool and are moved through the specimen by means of the movement of the laser spot with respect to time.

The decrease in the temperature profile along the weld pool surface results in an increase of the surface tension. Hence the molten material is accelerated away from the keyhole due to the produced shear stresses. As it can be seen, the regions on the upper and lower side in front of the keyhole caused by the Marangoni force are very small in comparison to those behind the keyhole. That can be easily explained by the difference in the amount of molten material in the two areas.

The calculated velocity of the molten metal within the weld pool is very small compared to the maximum velocity calculated at the free surfaces. The simulation results show that the influence of the natural convection on the weld bead geometry can be neglected.

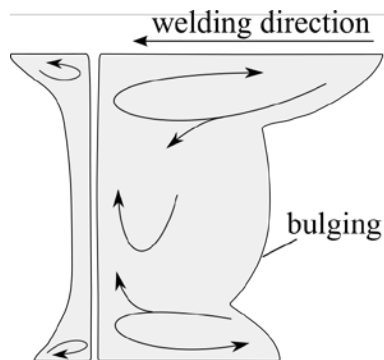


Fig. 5 Schematic view of the main flow directions in the molten pool from the symmetry plane of the model.

The shape of the middle part is mainly formed by the bulge of the keyhole and the high processing speed. The steady-state weld pool shape represents a mass equilibrium defined by the moving laser spot and the solidification speed at the rear side of the weld pool. Due to the movement of the laser spot new material is molten and added to the melt pool and due to cooling of the part, a certain amount of the molten material solidifies.

Trivially, in a case where the flow of the molten metal is neglected, the rear edge of the weld pool will be a simple parallel shift of the keyhole edge caused by the moving laser spot. In the upper and lower regions of the present model, where the Marangoni force dominates, cooler material is driven back to the vicinity of the keyhole to ensure the conservation of mass, causing the necking areas, see Fig. 4.

The combination of the Marangoni driven flow and the movement of the laser spot, which is moving away from the solidification front, results in the so-called bulging-region in the middle of the depth of the weld pool, see Fig.3 and Fig. 4.

#### 4. Conclusion

In this study, a special butt configuration of structural steel and transparent quartz glass was used to monitor and analyse the weld pool geometry in the longitudinal direction. A formation of a bulging-region in the middle of the thickness of the plate was observed. Its shape and dimensions were monitored with high-speed camera and an infrared camera system. The obtained results were analysed by help of numerical modelling of the laser beam welding process. The main factors playing a crucial role in the formation of the bulging-region were identified, namely the thermo-capillary driven flow at the upper and lower surfaces, caused by the difference in the temperature dependent surface tension and the movement of the laser source with respect to time.

#### Acknowledgements

Financial funding of the Deutsche Forschungsgemeinschaft (DFG, German Research Foundation) under Grant No. BA 5555/1-1 is gratefully acknowledged.

This work was supported by the Research Association for Steel Application (FOSTA), the Federation of Industrial Research Associations (AiF) and the German Federal Ministry for Economic Affairs and Energy, (BMWi Bundesministerium für Wirtschaft und Energie), (Project 19582N, ‘Investigation of influence the restraint conditions on hot cracking in laser and laser-hybrid welding of thick structure steels’).

#### References

- [1] Bachmann, M., Gumenyuk, A., & Rethmeier, M. (2016). Welding with high-power lasers: trends and developments. *Physics Procedia*, 83, 15–25.
- [2] Zhang, X., Ashida, E., Tarasawa, S., Anma, Y., Okada, M., Katayama, S., & Mitzutani, M. (2011). Welding of thick stainless steel plates up to 50 mm with high brightness lasers. *Journal of Laser Applications*, 23(2), 022002.
- [3] Ready, J. F., & Farson, D. F. (Eds.). (2001). *LIA handbook of laser materials processing*. Orlando: Laser Institute of America.
- [4] Gebhardt, M., Gumenyuk, A., & Rethmeier, M. (2013). Numerical Analysis of Hot Cracking in Laser-Hybrid Welded Tubes. *Advances in Material Science and Engineering*.
- [5] Cho, W. I., Na, S. J., Thomy, C., & Vollertsen, F. (2012). Numerical simulation of molten pool dynamics in high power disk laser welding. *Journal of Materials Processing Technology*, 212(1), 262–275.
- [6] Sohail, M., Han, S. W., Na, S. J., Gumenyuk, A., & Rethmeier, M. (2015). Numerical investigation of energy input characteristics for high-power fiber laser welding at different positions. *The International Journal of Advanced Manufacturing Technology*, 80(5–8), 931–946.
- [7] Li, S., Chen, G., Zhang, M., Zhou, Y., & Deng, H. (2014). Investigation of keyhole plasma during 10 kW high power fiber laser. *Laser Physics*, 24, 106003.
- [8] Zhang, Y., Li, S., Chen, G., Zhang, H., & Zhang, M. (2012). Characteristics of zinc behavior during laser welding of zinc “sandwich” sample. *Optics & Laser Technology*, 44, 2340–2346.
- [9] Bachmann, M., Avilov, V., Gumenyuk, A., & Rethmeier, M. (2011). Numerical simulation of full-penetration laser beam welding of thick aluminium plates with inductive support. *Journal of Physics D: Applied Physics*, 45(3), 035201.
- [10] Artinov, A., Bachmann, M., & Rethmeier, M. (2018). Equivalent heat source approach in a 3D transient heat transfer simulation of full-penetration high power laser beam welding of thick metal plates. *International Journal of Heat and Mass Transfer*, 122, 1003–1013.
- [11] J. Larsson, Numerical Simulation of Turbulent Flows for Turbine Blade Heat Transfer, Doctoral Thesis for the Degree of Doctor of Philosophy, Chalmers University of Technology, Sweden, 1998.
- [12] Faber, T. E. (1995). *Fluid dynamics for physicists*. Cambridge University Press.
- [13] Brent, A. D., Voller, V. R., & Reid, K. T. J. (1988). Enthalpy-porosity technique for modeling convection-diffusion phase change: application to the melting of a pure metal. *Numerical Heat Transfer, Part A Applications*, 13(3), 297–318.
- [14] Wilcox, D. C. (1998). *Turbulence modeling for CFD* (Vol. 2, pp. 103–217). La Canada, CA: DCW industries.
- [15] Kays, W. M. (1994). Turbulent Prandtl number—where are we?. *Journal of Heat Transfer*, 116(2), 284–295.
- [16] Hashemi, H. T., & Sliepcevich, C. M. (1967). A numerical method for solving two-dimensional problems of heat conduction with change of phase. In *Chem. Eng. Prog. Symp. Series* Vol. 63, No. 79, pp. 34–41.